Synthesis of an Evolutionary Fuzzy Multi-objective Energy Management System for an Electric Boat

Antonino Capillo[a], Enrico De Santis[b], Fabio Massimo Frattale Mascioli[c] and Antonello Rizzi[d]
Department of Information Engineering, Electronics and Telecommunications,
University of Rome "La Sapienza", Rome, Italy

Keywords: Energy Management System, Fuzzy System, Evolutionary Computation, Genetic Algorithm, Electric Vehicle, e-Boat.

Abstract: Even though it is known that Renewable Energy Sources (RESs) are necessary to face Climate Change and pollution, technology is still in a developement phase, aiming at improving energy exploitation from RESs, as these type of sources suffer from low energy density and variability over time. Thus, proper ICT infrastructures equipped with a robust software, i.e., Energy Management System (EMS), are needed to ensure that Renewable Energy (RE) does not go to waste. Relatively small local electrical grids called Microgrids (MGs) represent the EMS ecosystem, since their main features are the proximity between generation and loads and the presence of Energy Storage Systems (ESSs) adopted to recover surplus energy. The Vehicle-to-Grid (V2G) paradigm helps to realize the Smart City, which in substance is an interconnection of MGs hosting electrical vehicles for an efficient energy management at a larger scale. In this context, e-boats have only recently been considered. Hence, in this work a Multi-Objective (MO) EMS is synthesized for an e-boat docked in a small Microgrid (PV generator and ESS) with the aim of maximizing the charging time of the e-boat ESS and spending as little as possible both for energy purchase and also in terms of ESS wear. A Fuzzy Inference System - Hierarchical Genetic Algorithm (FIS-HGA) is used to achieve the Pareto Front, with the HGA that is in charge of optimizing the FIS parameters. Results laid to a balanced trade-off between the two objectives, since the e-boat ESS is almost fully charged in a reasonable time and with a low cost, compatible with people transportation. Last but not least, the inference process of a FIS is easily interpretable, in the perspective of an Explainable AI.

1 INTRODUCTION

Renewable Energy Sources (RESs) become a reference for Humankind day by day, being the RESs energy production increased since 2010, with a rise estimation of about 2.7 times by 2025 (Ellabban et al., 2014). Nevertheless, some critical aspects of RESs must be taken into account, aiming at a sustainable clean energy exploitation. First of all, RESs energy density is very small, if compared to fossil fuels (Layton, 2008). Secondly, RESs are very variable over time, such that it is difficult to predict clean energy generation. Since a sustainable energy generation comes with efficiency and stability, the aforementioned issues deserve a lot of attention. Operators do not have control over the RESs generation because it depends on geographic location (e.g. it is very difficult to produce enough solar energy in the shade of an hill); moreover, assuming to be in a energy-profitable location, even though PV generators are modular, the area occupied by panels could not be enough extended either for geographical, economical or space issues. If, in addition, the unpredictable nature of RESs is taken into account, it can be stated that RESs energy is precious and not even a kWh must be wasted. As a consequence, it is logical to install RESs generators as mush close as possible to the loads (es. PV panels on the roof of a residential building), with the purpose of avoiding energy transportation losses, in contrast with centralized energy generation (e.g. thermoelectric power plants), which consists in high energy density and power plants remote locations. According to the above logic, also saving excess clean energy is mandatory, so Energy Storage Systems (ESSs), are needed. That leads to relatively small electrical grids or Microgrids (MGs) that fundamentally consist of RESs generators and load, which are close together,

[a] https://orcid.org/0000-0002-6360-7737
[b] https://orcid.org/0000-0003-4915-0723
[c] https://orcid.org/0000-0002-3748-5019
[d] https://orcid.org/0000-0001-8244-0015

Capillo, A., De Santis, E., Mascioli, F. and Rizzi, A.
Synthesis of an Evolutionary Fuzzy Multi-objective Energy Management System for an Electric Boat.
DOI: 10.5220/0011527800003332
In *Proceedings of the 14th International Joint Conference on Computational Intelligence (IJCCI 2022)*, pages 199-208
ISBN: 978-989-758-611-8; ISSN: 2184-2825

ESSs and a link to the Main Grid for service stability (Badal et al., 2019). That said, even if energy losses can be avoided, efficiency must further be improved. In fact, if it was possible to predict RESs energy generation with enough accuracy, energy flows between the MG nodes could be optimized. For example, assuming that the ESS is completely discharged, if PV generation in the current hour was much larger than load demand and, according to the future hour prediction, PV generation was close to zero, it could be better to store the current-hour excess energy in the ESS than to sell it to the Main Grid for profit, since in the next hour it would be necessary to buy energy from the Main Grid, generally at a much higher price than in the current hour. In other words, thanks to an accurate prediction, it was chosen to store energy for future consumption, being that the best one among the available alternatives: an optimization task is performed. Thus, when the problem at hand counts much more variables and bounds, a proper prediction and optimization software, the Energy Management System (EMS) software, is needed for MG optimal energy flows (Duman et al., 2021). In the MGs context, Zero Emission Vehicles (ZEVs) ed hybrid vehicles can be seen as nodes, since they can store energy in their inner ESS and also provide energy to a MG (for example, a residential building) (Slama, 2021). Consequently, with the ZEVs and hybrid vehicles market expansion, it is interesting to synthesize EMS algorithms that also consider this kind of nodes. Even if many works in literature treat ZEVs or hybrid vehicles energy management in MGs (Alsharif et al., 2021), research about electric or hybrid boats is relatively young (Balestra and Schjølberg, 2021). With reference to works focused on e-boats or hybrid boats themselves, (Rafiei et al., 2021) considers fuel consumption and battery State of Charge (SoC), aiming at maximizing energy efficiency. In the context of MGs, (Özdemir et al., 2021) is very interesting, as it takes into account a set of docked hybrid boats. More in detail, the dock consists of RESs generators, Main Grid link and an Hydrogen storage unit while each boat is equipped with a fuel cell and an ESS. The overall cost for charging the hybrid boats (e.g. the purchased energy cost from the Main Grid) is minimized.

Both for building and docked e-boats EMSs (Xiang and Yang, 2021),(Hafiz Abdul Muqeet et al., 2021), Computational Intelligence (CI) and Machine Learning (ML) techniques are often preferred to exact algorithms for a reasonably faster problem solving, specially when the problem at hand is very complex. Particle Swarm Optimization (PSO) (Pozna et al., 2022), Evolutionary Computation (EC) algorithms (Capillo et al., 2018), Artificial Neural Networks (ANNs) (Zamfirache et al., 2022) and Market-Based algorithms (Palm, 2004) are among the most relevant paradigms. Particularly relevant is the Explainable AI topic (Li et al., 2022), according to which AI should provide explanations about the way it solves a problem, just like a human would do. This way, AI could be more reliable. Some works like (De Santis et al., 2013), (De Santis et al., 2017) rely on Fuzzy Logic for achieving grey-box AI models, since Term Sets and Fuzzy Rules try to replicate human consciousness during problem solving.

In this work, a Multi-Objective (MO) optimization problem for a docked full electric boat equipped with a PV roof and an ESS is faced, where Pareto Front (PF) trade-off solutions are found aiming at recharging the e-boat ESS as soon as possible and at minimizing costs. The PV-roof e-boat model and the dock design come from the "LIFE for Silver Coast" European Project (LIFE16 ENV/IT/000337), hereinafter referred to as "LIFE Project", whose aim is to realize a sustaitnable mobility system in Tuscany (IT) only with electrical vehicles. An AI "explainable" grey-box EMS, the Fuzzy Inference System - Hierarchical Genetic Algorithm (FIS-HGA) is synthesized, based on a FIS whose parameters are optimized by a Genetic Algorithm (GA). The purpose is to synthesize a grey-box AI model for this specific application. The EMS design is presented in Sec. 2; the dataset and the problem formulation are shown in detail in Sec. 3 and Sec. 4, respectively; the optimization procedure is explained in Sec. 5; the algorithm tests and results are presented in Sec. 6.

2 EMS DESIGN

2.1 The MG Architecture

In this section, the MG architecture is defined, together with a simplified version, considering some assumptions described below.

2.1.1 The Basic MG Architecture

The basic MG architecture, as shown in Fig. 1, represents the docked e-boat with the engine off, in the generic timeslot k. On the left side, all the dock elements are enclosed in an orange rectangle, while the elements related to the e-boat are enclosed in a green rectangle.

Node N represents the Main Grid, G is the PV generator, S is the dock ESS, $S^{'}$ is the e-boat ESS and $G^{'}$ is the e-boat PV roof. The elements named as BMS and EMS stand for "Battery Management System" and

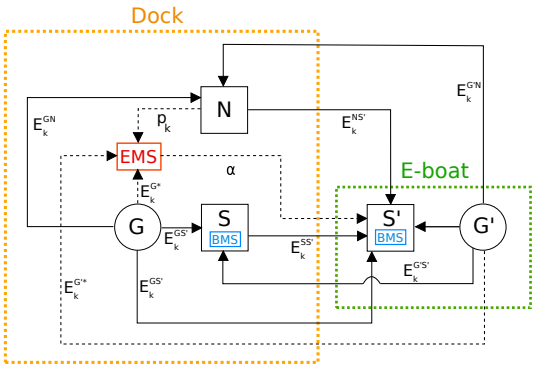

Figure 1: The basic MG architecture.

"Energy Management System", respectively. Square nodes are bidirectional, since energy can both flow from and to them. Circle nodes can only provide or receive energy from other nodes. Regardless a node is bidirectional or not, it can not both absorb/store energy from or generate/provide energy to the other nodes, in the same timeslot k. The BMS, which measures the State of Energy (SoE) of the ESS, is simulated in a workstation, running also the FIS optimization procedure. Energy flows are drawn as solid black lines in Fig. 1. The amount of energy which flows from the generic node i to the generic node j is indicated as E_k^{ij}. Thus, for example, $E_k^{NS'}$ is the amount of energy which flows from N to S', during timeslot. The nodes G and G' primarily meet the energy needs of S'. In fact, conveying energy from S, assuming that the dock ESS had been charged by G or G', would involve an additional operational cost due to the dock ESS wear. Furthermore, it would be useless to route the energy produced by G or G' to the Main Grid, since that energy is primarily necessary to the e-boat ESS. As a consequence, S and N should not receive energy from S' but only from G and G'. The MG information flows, drawn as dotted black lines in Fig. 1, are the following: the whole energy produced by G in the generic timeslot E_k^{G*}, the whole energy produced by G' in the generic timeslot $E_k^{G'*}$, the Main Grid energy purchase price p_k and the EMS decision variable α, which controls whether S' receives the difference between its energy demand and the whole PV production (G and G') from N or from S. It is assumed that suitable smart meters collect the above mentioned information.

2.1.2 Simplified MG Architecture

According to the aforementioned considerations, S', G and G' can be grouped in a single node $S'G'G$, as in 2. Thus, the overall PV energy production in the

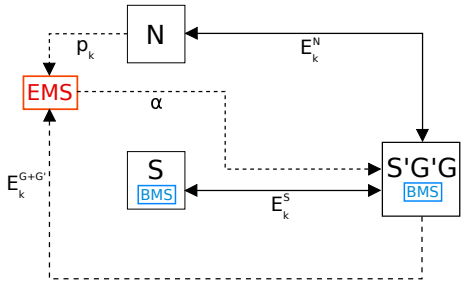

Figure 2: The simplified MG architecture.

generic timeslot $E_k^{G+G'}$ and p_k are the two inputs of the EMS and the decision variable α is the system output.

2.2 System Objectives

The EMS is in charge of optimizing the MG energy flows for achieving both the minimum overall charging cost and the minimum charging time of the e-boat ESS. The quicker the charging process is, the more stressed the ESS will be and, as a consequence, the more expensive the charging process will be because of the ESS wear cost. Moreover, the quicker the charging process is, the higher the probability of buying energy from the Main Grid in k is, since S, G and G' could not provide enough energy to meet the e-boat demand. For the above reasons, the presented objectives are in contrast to each other, hence the one at hand is a Multi-Objective Pareto Front problem to face.

2.3 MG Sizing

According to the LIFE Project, the area dedicated to the PV panels is about 15 [mq]. Thanks to the European Commission PVGIS tool (EC, 2020), an estimation of the PV generator peak power can be done by the (1):

$$P = 1\frac{kWp}{m^2} A\,\eta \qquad (1)$$

where P is the PV generator peak power, in [kWp]; A is the area dedicated to the PV panels, in [mq] and η is the PV panels efficiency. The (1) is generally used to assess the PV panels peak power when it has been not provided by the manufacturer yet. Thus, the peak power is calculated assuming that the PV panels generate a fraction (given by the efficiency) of the power it would generate under the Standard Conditions (i.e. 1000 W/m2 solar irradiance, a module temperature of 25° C and a solar spectrum corresponding to an air mass of 1.5). As specified in (Departement of Energy, 2016), the crystalline Silicon PV panels effi-

ciency is about 0.25 for single-crystal cells while is roughly 0.20 for multi-crystalline cells. With the aim of exploiting solar irradiation well throughout the day, multi-crystalline cells are to be preferred so that η is set to 0.20. Therefore, the PV generator peak power is 3 [kWp]. By a similar reasoning, the e-boat PV roof peak power is about $1,5$ [kWp], since the area of the PV panels is 8 [mq]. The dock ESS capacity is set to be equal to the e-boat ESS capacity, which is designed to be 50 [kWh]. This choice guarantees that the e-boat ESS could be always fully charged when docked, being the initial dock ESS SoE the 80% of its capacity while the initial e-boat ESS SoE the 20% of the same quantity. The ESS (both for dock and e-boat) charging/discharging energy bound is set to 5 [kWh], according to the Tesla Powerwall technical features (Tesla, 2019).

3 DATASET

The dataset consist in hourly PV generation and Main Grid energy purchase prices figures for 2020. More detailed information about data and sources are reported below.

3.1 PV Generation

Through the PVGIS tool (EC, 2020), it is possible to achieve an estimation of the hourly PV production data for a given geographic position, which for the LIFE Project is $44.442°N, 11.215°W$ (Orbetello, Tucany, IT). PVGIS tool input values for the dock PV generator include the peak power of about 3 kWp, system loss (e.g. from cables) of about 14% and slope/azimuth figures.
In particular, system loss (for example, losses in cables, power inverters and dirt on the PV modules) together with the Slope (angle of the PV modules from the horizontal plane) are set by default, while the Azimuth (the angle of the PV modules relative to South) is set for a perfect orientation to South. PVGIS tool input values for the dock PV generator include the peak power of about 1.5 kWp, system loss (e.g. from cables) of about 14% and slope/azimuth figures,
whereslope is set to 0 degrees because the e-boat PV roof is in a fixed position, parallel to the deck.

3.2 Energy Purchase Prices

The Main Grid energy purchase prices come from the Open Power System Data (Zürich, 2020). More precisely, data pertain the Center of Italy (where the LIFE Project area is located), for 2020.

3.3 Dataset Analysis

Figures about energy purchase prices for 2020 are available only until 1^{st} October 2020, therefore, the dataset consists of nine months of data, until the end of September 2020. Since the e-boat is designed to operate mainly during peak season, the dataset timespan is acceptable. No other lack of data is observed.

4 PROBLEM FORMULATION

The problem formulation consists of the following equations:

$$\min_{k,\alpha\ \varepsilon\ \mathbb{R}} \sum_{k=1}^{T} \frac{(1-SoE'_k)}{T}, \tag{2}$$

$$\min_{k,\alpha\ \varepsilon\ \mathbb{R}} \sum_{k=1}^{T} \frac{(w_k^{S'} + w_k^{S} + c_k^{buy})}{T} \tag{3}$$

where:

$$T \geq k \geq 0 \tag{4}$$

$$1 \geq \alpha \geq 0 \tag{5}$$

$$1 \geq SoE'_k \geq 0 \tag{6}$$

$$1 \geq SoE_k \geq 0 \tag{7}$$

$$w_k^{S'} = \left(\frac{SoE'_k - 0.5}{0.5}\right)^{12} \tag{8}$$

$$w_k^{S} = \left(\frac{SoE_k - 0.5}{0.5}\right)^{12} \tag{9}$$

$$c_k^{buy} = \begin{cases} 0 & if \quad E_k^N \leq 0 \\ p_k E_k^N & if \quad E_k^N > 0 \end{cases} \tag{10}$$

$$E_k^N + E_k^S + E_k^{S'GG'} = 0 \tag{11}$$

$$E_k^{S'} = \begin{cases} \alpha \frac{E_k^{S'max}}{0.49} - E_k^{S'max} & if \quad \alpha \leq 0.49 \\ (\alpha - 0.50)\frac{E_k^{S'max}}{0.50} & if \quad \alpha \geq 0.50 \end{cases} \tag{12}$$

$$E_k^N = \begin{cases} -E_k^{S'GG'} & if \quad \alpha \leq 0.49 \\ & and \quad |E_k^{S'GG'}| < E_{Smax} \\ E_{Smax} - |E_S| & if \quad \alpha \geq 0.50 \\ & and \quad |E_k^{S'GG'}| \geq E_{Smax} \\ 0 & if \quad \alpha \geq 0.50 \\ & and \quad |E_k^{S'GG'}| < E_{Smax} \end{cases} \tag{13}$$

$$E_k^S = \begin{cases} 0 & if \quad \alpha \leq 0.49 \\ -E_k^{S'GG'} & if \quad \alpha \geq 0.50 \\ & and \quad |E_k^{S'GG'}| < E_{Smax} \\ -E_{Smax} & if \quad \alpha 1 \geq 0.50 \\ & and \quad |E_k^{S'GG'}| \geq E_{Smax} \end{cases} \tag{14}$$

$$E_k^{S'max} = E_k^{Smax} = 5 \tag{15}$$

$$C' = C = 50 \tag{16}$$

$$SoE'_k = SoE'_{k-1} - \frac{E_k^{S'}}{C'} \tag{17}$$

$$SoE_k = SoE_{k-1} - \frac{E_k^{S}}{C} \tag{18}$$

The EMS minimizes two Objective Functions (OFs). The fist OF, given in (2), is the sum of the e-boat ESS capacity fractions that are full of energy, over the whole dataset (T is the total number of timeslots k and SoE'_k is the e-boat ESS State of Energy, bounded as in (6). Minimizing the OF (2) means maximizing the number of timeslots the e-boat ESS is full, i.e. minimizing the ESS charging time. The second OF is the sum of the overall MG costs over the whole dataset, i.e. the e-boat ESS wear cost $w_k^{S'}$ given by (8), the dock ESS wear cost w_k^S given by (9) and the Main Grid energy purchase c_k^{buy} given by (10). The ESS wear cost formulation comes from (Ferrandino et al., 2020) such that the more the SoE deviates from the 50% of the capacity the more the battery is stressed. The energy purchase cost is considered everytime there is an energy flow from the Main Grid, that fore every k where E_k^N is positive. In fact, conventionally, a positive amount of energy for a given node of the MG means that it is providing energy, while a negative amount means that it is receiving energy. Thus, when E_k^N is positive, c_k^{buy} is the product of E_k^N for the energy purchase price at k. The MG energy balance is guaranteed by (11). The EMS output (or decision variable) α is a real-valued number that is rounded to the second decimal place. It is in charge of deciding both the amount of energy to store in the e-boat ESS in k, as shown in (12), and the node the e-boat ESS can mainly receive energy from, by (13) and (14). More precisely, if α is less than or equal to 0.49, the e-boat ESS stores energy never over its technical limit ($E_k^{S'max}$) by (12) and it charges itself primarily from G and G' before relying on N by (13) (i.e. $E_k^{S'GG'}$ is negative). With the aforementioned condition on α in k, S does not exchange any energy. On the other hand, if α is greater than or equal to 0.50, the e-boat ESS stores energy never over its technical limit (E_k^{Smax}) by (12) and it charges itself primarily from G and G' before relying on S by (14) (i.e. $E_k^{S'GG'}$ is negative). That said, if the amount of energy $E_k^{S'GG'}$ exceeds E_k^{Smax}, the difference between the former and the latter is provided by N, by (13). With similar reasoning, again by (13) and (14), S and N receive energy from $S'G'G$, if the energy balance of the former is positive. The values of $E_k^{S'max}$ and E_k^{Smax} are set by (15), according to Section 2.3, as it is for the ESSs capacity, by (16). Furthermore, timeslot by timeslot, the SoE of the ESSs is updated by (17) and (18).

5 THE FIS-GA OPTIMIZATION

In a FIS-GA optimization (De Santis et al., 2013), (De Santis et al., 2017), the FIS parameters are properly set by a GA to achieve the problem objectives. In the following, more details are given about the optimization procedure performed in this work. According to the FIS-HGA paradigm (De Santis et al., 2017), the GA can control which Rules to delete in the Rule Base. This feature is useful fore achieving the core of the most relevant Rules for the problem at hand. Each one of these new Genes represents the presence or absence of a MF such that, if the MF is absent, the Rules with that MF are deleted. The aforementioned Genes are called Hierarchical Genes. The generic HGA Individual can be represented as follows:

$$I_h = [\vec{g_h},\ \vec{g_a},\ \vec{g_{MF}},\ \vec{g_c},\ \vec{g_w}] \tag{19}$$

where $\vec{g_h}$ is the vector of the binary Hierarchical Genes, $\vec{g_a}$ is the vector of Antecedents, $\vec{g_M F}$ encodes the MF abscissas, $\vec{g_c}$ is the vector of Consequents and $\vec{g_h}$ encodes Rule Weights.

5.1 Design of the MO-FIS-HGA Algorithm

5.1.1 Optimization Workflow

A MO-FIS-HGA optimization algorithm returns the optimal FIS models that belong to the Pareto Front. In fact, as specified in Subsection 2.2, two OFs, in contrast to each other, are considered. The optimization workflow is presented in Fig. 3.

5.1.2 FIS Design

A Mamdami-type FIS consists of 25 Rules in the Rule Base and a five MFs Term set, for both the two Inputs

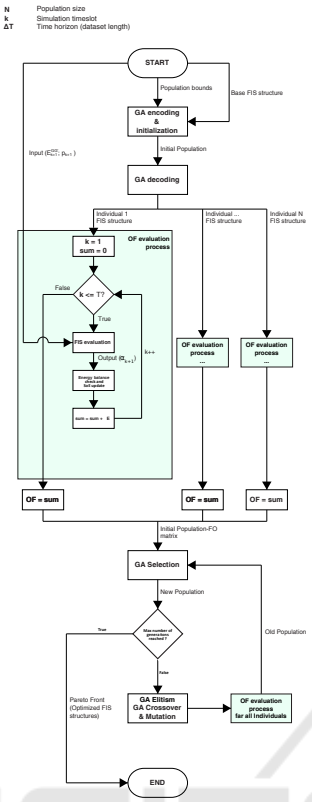

Figure 3: Optimization flowchart.

and the Output. The number of Rules comes from (20):

$$n_R = n_{MFs}^{n_{In}} \tag{20}$$

where n_R is the number of Rules, n_{In} is the number of Inputs (2, in this case) and n_{MFs} is the number of MFs in the Term Set (5 in this case).

5.1.3 HGA Design

The MO-HGA encodes Consequents and Weights as Genes of its Individuals and the generic current Population evolves, generation by generation, with the aim of finding a PF trade-off between the two OFs. Inspired by (Dietz et al., 2008), at first, the GA finds the Individuals with the minimum values of the two OFs. This Elitism procedure aims at covering the PF edges. Then, two Selection processes are performed: the first one, considering the first OF and the second one considering the second OF. That leads to achieve two groups of Individuals: the first one, containing Individuals from the first Selection (i.e. with good values for the first OF); the second one, as large as the first one, containing Individuals from the second Selection (i.e. with good values for the second OF), finally performing a crossover between the Individuals of the aforementioned groups. This practice 'breeds' Individuals in a way that, Generation by Generation, the probability that they will reach the inner part of the Pareto Front increases. Then, Mutation is applied to remaining Individuals of the current Population, leading to the updated Population completion and, thus, to a new Generation. The HGA operators and meta-parameters, which are set by the operator based on previous experience on this kind of applications, are shown in Tab. 1.

Table 1: HGA operators and meta-parameters.

Figure	Value
Pop. size	300
Elite Indiv.	1 (per OF)
Selection Op.	Tournament
Sel. Tour. size	2
Mutation Op.	Uniform
Mut. Fraction	0.2
Crossover Op.	One-point
Cros. Fraction	0.8
Stopping cond.	Max. Gen.
Max Gen.	50

FIS MFs abscissas are encoded as Genes but further transformations are done with the aim of reducing the number of Genes and, therefore, the computational cost. First of all, the UoD is discretized with 0.01 steps. Then, MFs abscissas are encoded following the (21 - 35) . With reference to Fig. 4, even if each triangular MF counts three abscissas, only two real values are needed, according to the aforementioned equations and inequalities.

$$\gamma = g'_{verylow}\,\gamma_0 \tag{21}$$

$$\beta = g''_{verylow}\,\gamma \tag{22}$$

$$\theta = g'_{veryhigh}\,(1-\theta_0) \tag{23}$$

$$\lambda = \theta + g''_{veryhigh}\,(1-\theta) \tag{24}$$

$$\phi = \begin{cases} \phi_0 - (\frac{g'_{low}}{2} L_{low} - \frac{L_t r}{2}) & if \quad g'_{low} \geq 1 \\ \phi_0 + (-\frac{g'_{low}}{2} L_{low} + \frac{L_t r}{2}) & if \quad 0.01 \geq g'_{low} < 1 \end{cases} \tag{25}$$

$$\xi = \begin{cases} \xi_0 + (\frac{g''_{low}}{2} L_{low} - \frac{L_t r}{2}) & if \quad g'_{low} \geq 1 \\ \xi_0 - (-\frac{g''_{low}}{2} L_{low} + \frac{L_t r}{2}) & if \quad 0.01 \geq g'_{low} < 1 \end{cases} \tag{26}$$

$$\omega = \phi + g''_{low}\,\frac{(\xi - \phi)}{2} \tag{27}$$

with

$$\gamma_0 = 0.25 \tag{28}$$

$$\theta_0 = 0.75 \tag{29}$$

$$0.04 \geq g'_{verylow} \leq 4.00 \tag{30}$$

$$0.01 \geq g''_{verylow} \leq 0.99 \tag{31}$$

$$0.04 \geq g'_{veryhigh} \leq 4.00 \tag{32}$$

$$0.01 \geq g''_{veryhigh} \leq 0.99 \tag{33}$$

$$0.01 \geq g'_{low} \leq \frac{1}{L_{tr}} \tag{34}$$

$$0.01 \geq g''_{low} \leq 1.99 \tag{35}$$

where γ, β, θ, λ, ϕ, ξ and ω are the MFs abscissas (Fig. 4), being γ_0, β_0, θ_0, λ_0, ϕ_0, ξ_0 and ω_0 their default values; $g'_{verylow}$ and $g''_{verylow}$ are the first and the second Genes for the "very low" trapezoidal MF, respectively; $g'_{veryhigh}$ and $g'_{veryhigh}$ are the first and the second Genes for the "very high" trapezoidal MF, respectively; g'_{low} and g''_{low} are the first and the second Genes for the "low" triangular MF, respectively. The "low" triangular MF is to be considered representative of the others triangular MFs; thus, for the sake of the synthesis, the values of ϕ_0, ξ_0 and ω_0 are omitted in the equations above. The equations and inequalities above guarantee MFs abscissas variations over the whole UoV also preventing overlaps. This way, the number of MFs abscissas Genes is 30 (3 overall Terms Sets - for 2 Inputs and 1 Output - for 5 MFs per Term Set for 2 Genes per MF) instead of 39 (3 overall Terms Sets - for 2 Inputs and 1 Output - for 5 MFs per Term Set for 2 Genes per trapezoidal MF and 3 Genes per triangular MF.).
As discussed above, the generic Individual counts 90 Genes: 10 Hierarchical Genes (1 per Input MF for 5 MFs per per Input Term Set for 2 Input Term Sert); 30 MFs Genes; 25 Consequents Genes (1 per Rule for 25 Rules); 25 Weight Genes(1 per Rule for 25 Rules).

5.2 Benchmark and Performance Metrics

A Dynamic Programming (DP) algorithm is used as benchmark in this work. According to Literature (Kim and de Weck, 2005), (Koski, 1985), a benchmark PF can be achieved by implementing a mono-objective algorithm with a single weighted-sum OF, by finding problem solutions for many different weights values. In this work, 100 different benchmark PF points are achieved by the above procedure.

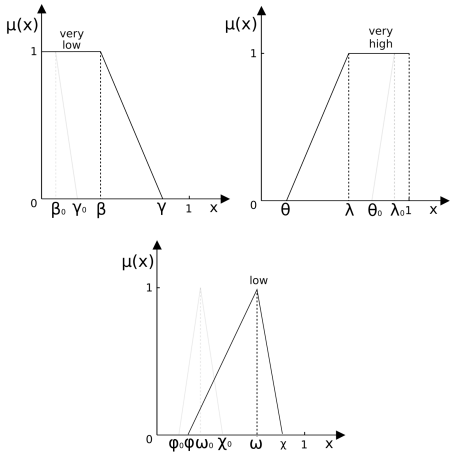

Figure 4: MF encoding scheme.

With regard to the performance metrics, the following criteria must be taken into account for a MO optimization (Chen et al., 2007), (Unveren and Acan, 2007):

- Proximity of the GA PF points the to the benchmark PF points;
- Coverage of the benchmark PF by the GA PF points;
- Distribution of the GA PF points.

Proximity can be estimated through the Generational Distance (GD) (Unveren and Acan, 2007), as follows:

$$GD = \sqrt{\frac{\sum_i^M z_i}{M}} \tag{36}$$

where z_i is the distance between the i-th GA PF point and its nearest benchmark PF point and M is the total number of GA PF points. If GD is 0, GA PF points overlap with the benchmark PF points.
Both coverage and distribution can be evaluated through the Diversity Metric (DM) (Chen et al., 2007), (Unveren and Acan, 2007), with reference to Fig. 5, as follows:

$$DM = \frac{d_b + d_e + \sum_i^{M-1} (d_i - \bar{d})}{d_b + d_e + (M-1)\,\bar{d}} \tag{37}$$

where d_b and b_e are the distance between the extreme GA PF points and the corresponding points in the benchmark PF, while d_i and $\bar{d}$ are the distance between two consecutive GA PF points and their mean value, respectively. It can be seen that the more the mutual distance between GA PF points is closer to $\bar{d}$ and the distances d_b and d_e are small, the more DM tends to 0, which means a perfect GA PF points covering and distribution.

According to (Chen et al., 2007) and (Unveren and Acan, 2007), values of GD up to about 0.45 and values of DM up to about 0.40 are acceptable.

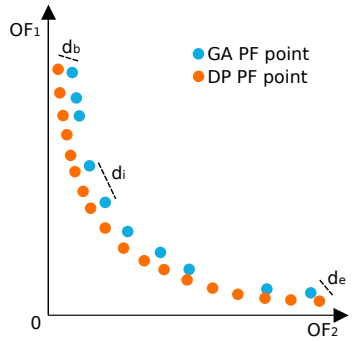

Figure 5: Density Metric (DM) calculation quantities.

6 TESTS AND RESULTS

In order to achieve the optimal FIS models with the best generalization skills, a k-fold cross-validation is performed by choosing 5 couples of days (5-fold) in the dataset trying to cover as much as possible the whole year. Therefore, each couple consists of one training day subset and one validation day subset and the PF solutions (i.e. the optimal FIS models) with the minimum validation error are selected before being tested on one day, randomly chosen in the dataset. More precisely, the error ε is calculated as the sum of GD and DM performance metrics (38), aiming at guaranteeing both accuracy and a good PF points distribution. In fact, the aforementioned sum of performance metrics acts as weighted-sum objective function with equal given both to GD and DM, aspiring at a good compromise result.

$$\varepsilon = GD + DM \tag{38}$$

The result of the learning process is the optimal GA PF, which consists of the best FIS models for the problem at hand. The optimal GA PF is plotted against the benchmark PF in Fig. 6 and figures about the algorithm performance are reported in Tab. 2. Since the GA is a stochastic algorithm, the values in Tab. 2 are calculated as averages over 10 runs.

At the best of our knowledge, the proposed algorithm achieves acceptable results in GD figures but also promising values of DM, if compared to other GA-based algorithms (Unveren and Acan, 2007), (Chen et al., 2007). That could be encouraging for further improvements of the model.

For three GA PF points, (i.e. FIS models), the resulting optimal energy flows are extracted and shown in Fig. 7, together with an estimation of the energy purchase cost from the Main Grid. The points are chosen

Table 2: MO-FIS-HGA performance metrics.

Figure	Mean	Variance
Train. GD	0.062	0.002
Train. DM	0.162	0.0013
Val. GD	0.076	0.009
Val. DM	0.162	0.004
Test. GD	0.063	0.009
Test. DM	0.164	0.009
Comp. cost [h]	6.320	0.005

to be the two extreme points of the PF and the one in the middle (Fig. 6) because in a MO optimization it is interesting to study both the sharp and the compromise solutions, in order to choose the most suitable one.

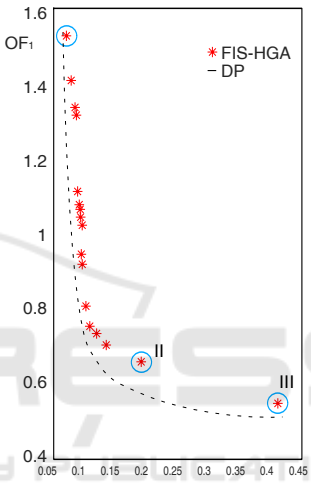

Figure 6: FIS-HGA Pareto Front selected points.

In the Point I case, for a faster e-boat ESS charge (about 2 hours), the dock ESS immediately transfers as much energy as possible to the e-boat ESS, according to its technical limits. The larger energy contribution comes from the Main Grid, with an energy purchase cost that is the higher among the overall cases. In the opposite case of Point III, a very smaller quantity of energy is absorbed by the e-boat from the Main Grid, with about a purchase costs less than about the 85%. Moreover, solar energy is exploited to charge both the e-boat ESS and the dock ESS. That makes it possible to buy less energy from the Main Grid than in the other cases and also to charge less rapidly, with a lower stress for the ESSs (it is better if an ESS SoE is around 50%). As a consequence, the e-boat ESS is not fully charged (about 90%) and it takes the whole day to finish charging. In a compromise solution, in the Point II case, the energy purchase costs are less than the 50% if compared to Point I case and at 12 o'clock it is almost fully charged (about 80%). The last case can be considered the best in terms of lo-

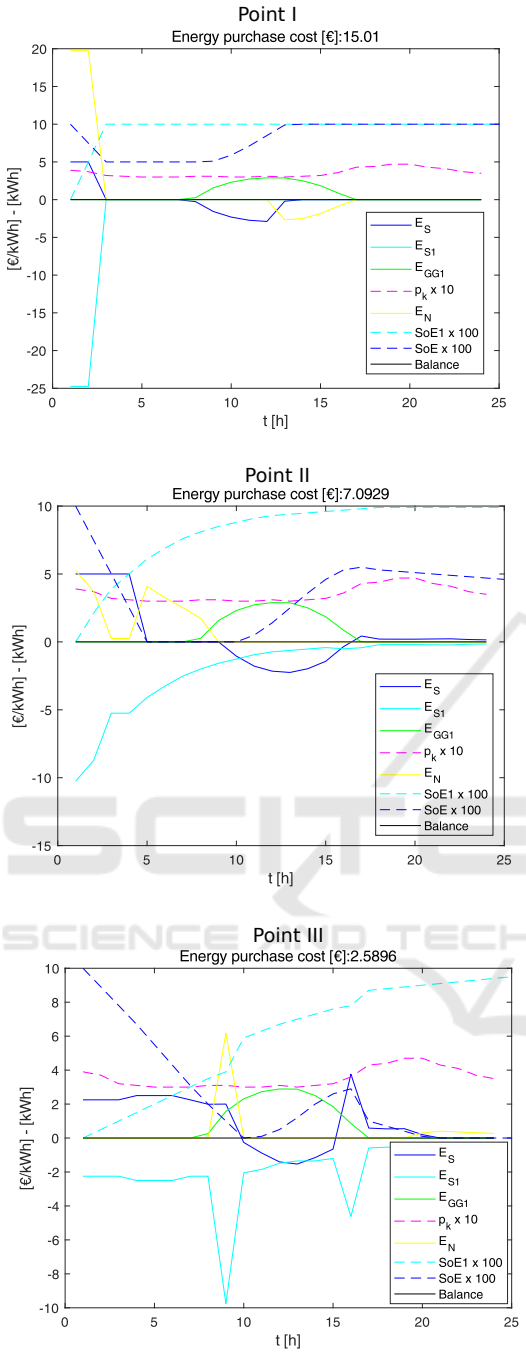

Figure 7: Optimal energy flows from delected FIS-HGA Pareto Front points.

gistic and economic points of view, so the first Input Term Set (as an example) of the corresponding FIS model (Fig. 8) are discussed below for the sake of the AI Explainability.

Together with the Rule Set (Fig. 9) the Term Sets make the FIS reasoning comprehensible to humans, in contrast with AI black-box models.

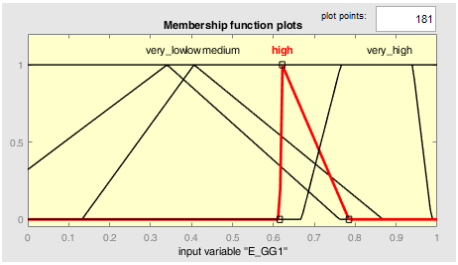

Figure 8: Point II FIS Term Set for the first Input.

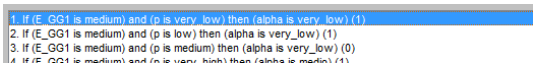

Figure 9: Point II FIS Rule Base excerpt.

7 CONCLUSIONS

An MO EMS is synthesized for a docked e-boat with the aim of optimizing two conflicting objective functions, i.e. charging the e-boat ESS as soon as possible within 24*h* and spending as little as possible both for energy purchase from the Main Grid and also in terms of ESS wear. A FIS-HGA algorithm is used to achieve the Pareto Front for evaluating compromise solutions. The HGA is in charge of optimizing the FIS parameters in order to return a FIS model that meets the needs. Five k-fold, each with one training and one validation day dataset, are considered for cross-validation. Results laid to a balanced trade-off between the two objectives, since the selected solution make it possible to charge the e-boat ESS in a reasonable time for people transportation services (it is almost fully charged at 12 o' clock) with an overall expenditure that is less than 50%, if compared to the most expensive solution. Having a FIS model as a function approximation model makes it possible to know its reasoning process by observing Term Set and Rule Base, since they are written in a Natural-like Language. The proposed algorithm achieves good results in DM figures while only acceptable figures in GD, if compared to literature. That could be encouraging for further improvements of the model. One of the model flaws is the high computational cost that requires efforts in writing more efficient code and in exploiting better parallel computation.

REFERENCES

Alsharif, A., Tan, C. W., Ayop, R., A.Dobi, and Lau, K. Y. (2021). A comprehensive review of energy management strategy in vehicle-to-grid technology integrated with renewable energy sources. *Sustainable Energy Technologies and Assessments*, 47:101439.

Badal, F., Das, P., and et al., S. S. (2019). A survey on control issues in renewable energy integration and microgrid. *Protection and Control of Modern Power Systems*, 4.

Balestra, L. and Schjølberg, I. (2021). Energy management strategies for a zero-emission hybrid domestic ferry. *International Journal of Hydrogen Energy*, 46(77):38490–38503.

Capillo, A., Luzi, M., Pasc, M., Rizzi, A., and Mascioli, F. M. F. (2018). Energy transduction optimization of a wave energy converter by evolutionary algorithms. In *2018 International Joint Conference on Neural Networks (IJCNN)*, pages 1–8.

Chen, L., McPhee, J., and Yeh, W. W.-G. (2007). A diversified multiobjective ga for optimizing reservoir rule curves. *Advances in Water Resources*, 30(5):1082–1093.

De Santis, E., Rizzi, A., and Sadeghian, A. (2017). Hierarchical genetic optimization of a fuzzy logic system for energy flows management in microgrids. *Applied Soft Computing*, 60:135–149.

De Santis, E., Rizzi, A., Sadeghiany, A., and Frattale Mascioli, F. M. (2013). Genetic optimization of a fuzzy control system for energy flow management in micro-grids. In *2013 Joint IFSA World Congress and NAFIPS Annual Meeting (IFSA/NAFIPS)*, pages 418–423.

Departement of Energy, U. (2016). Crystalline silicon photovoltaic research. http://www.energy.gov/eere/solar/crystalline-silicon-photovoltaics-research.

Dietz, A., Azzaro-Pantel, C., Pibouleau, L., and Domenech, S. (2008). Strategies for multiobjective genetic algorithm development: Application to optimal batch plant design in process systems engineering. *Computers & Industrial Engineering*, 54(3):539–569.

Duman, A. C., Erden, H. S., Ömer Gönül, and Önder Güler (2021). A home energy management system with an integrated smart thermostat for demand response in smart grids. *Sustainable Cities and Society*, 65:102639.

EC (2020). Photovoltaic geographical information system. http://re.jrc.ec.europa.eu/pvg_tools/en/.

Ellabban, O., H.Abu-Rub, and Blaabjerg, F. (2014). Renewable energy resources: Current status, future prospects and their enabling technology. *Renewable and Sustainable Energy Reviews*, 39:748–764.

Ferrandino, E., Capillo, A., Frattale Mascioli, F. M., and Rizzi, A. (2020). Nanogrids: A smart way to integrate public transportation electric vehicles into smart grids. In *12th International Joint Conference on Computational Intelligence*, volume 16.

Hafiz Abdul Muqeet, a. H. M. M., Javed, H., Shahzad, M., Jamil, M., and Guerrero, J. M. (2021). An energy management system of campus microgrids: State-of-the-art and future challenges. *Energies*, 14(20).

Kim, I. and de Weck, O. (2005). Adaptive weighted-sum method for bi-objective optimization: Pareto front generation. *Structural and Multidisciplinary Optimization*, 29(2):149–158.

Koski, J. (1985). Defectiveness of weighting method in multicriterion optimization of structures. *Communications in Applied Numerical Methods*, 1(6):333–337.

Layton, B. E. (2008). A comparison of energy densities of prevalent energy sources in units of joules per cubic meter. *International Journal of Green Energy*, 5:438–455.

Li, X.-H., Cao, C. C., Shi, Y., Bai, W., Gao, H., Qiu, L., Wang, C., Gao, Y., Zhang, S., Xue, X., and Chen, L. (2022). A survey of data-driven and knowledge-aware explainable ai. *IEEE Transactions on Knowledge and Data Engineering*, 34(1):29–49.

Palm, R. (2004). Synchronization of decentralized multiple-model systems by market-based optimization. *IEEE Transactions on Systems, Man, and Cybernetics, Part B (Cybernetics)*, 34(1):665–671.

Pozna, C., Precup, R.-E., Horvath, E., and Petriu, E. M. (2022). Hybrid particle filter-particle swarm optimization algorithm and application to fuzzy controlled servo systems. *IEEE Transactions on Fuzzy Systems*, pages 1–1.

Rafiei, M., Boudjadar, J., and Khooban, M.-H. (2021). Energy management of a zero-emission ferry boat with a fuel-cell-based hybrid energy system: Feasibility assessment. *IEEE Transactions on Industrial Electronics*, 68(2):1739–1748.

Slama, S. B. (2021). Design and implementation of home energy management system using vehicle to home (h2v) approach. *Journal of Cleaner Production*, 312:127792.

Tesla (2019). Pawerwall 2 datasheet. http://www.tesla.com/powerwall.

Unveren, A. and Acan, A. (2007). Multi-objective optimization with cross entropy method: Stochastic learning with clustered pareto fronts. In *2007 IEEE Congress on Evolutionary Computation*, pages 3065–3071.

Xiang, Y. and Yang, X. (2021). An ecms for multi-objective energy management strategy of parallel diesel electric hybrid ship based on ant colony optimization algorithm. *Energies*, 14(4).

Zamfirache, I. A., Precup, R.-E., Roman, R.-C., and Petriu, E. M. (2022). Reinforcement learning-based control using q-learning and gravitational search algorithm with experimental validation on a nonlinear servo system. *Information Sciences*, 583:99–120.

Özdemir, H., Güldorum, H. C., Erdinç, O., and İbrahim Şengör (2021). Energy management of a port serving fuel cell and battery based hybrid green ferries. In *2021 International Conference on Smart Energy Systems and Technologies (SEST)*, pages 1–6.

Zürich, E. (2020). Open power system data. http://data.open-power-system-data.org/time_series/.